M. Kovalenko[1,2], O. Bovgyra[1], V. Dzikovskyi[1,2], A. Kashuba[2], H. Ilchuk[2],
R. Petrus[2], I. Semkiv[2]

Effect of Al Doping on Optical Properties of ZnO Thin Films: Theory and Experiment

[1]Ivan Franko National University of Lviv, Lviv, Ukraine, mariya.kovalenko@lnu.edu.ua
[2]Lviv Polytechnic National University, Lviv, Ukraine, andriykashuba07@gmail.com

The structural, electronic, and optical properties of zinc oxide thin films with Al-doping have been investigated experimentally and with density functional theory (DFT) calculations. Changes in properties of doped thin films, which are deposited on a glass substrate by a high-frequency magnetron sputtering method, are monitored using X-ray diffraction data and UV measurements. Our theoretical calculations show that the electronic structure of ZnO: Al can be well described by the DFT+U method. The XRD measurements demonstrated the formation of a pure single ZnO phase and Al atoms is well incorporated in the ZnO lattice. Also, we determine the optical constants such as optical dielectric function, refractive index, optical band gap values, extinction coefficient, and optical conductivity of the doping films through transmittance spectra. The calculated results show the change of lattice parameters Al-doped ZnO. The optical band gap of ZnO: Al is increased compared with pure ZnO. Besides, around the Fermi level of Al-doped ZnO was emerged the shallow donor states from mainly 3s-Al states. Our DFT calculations of optical properties Al-doped ZnO agree satisfactorily with the experimentally measured transmittance values.

Keywords: Al-doped ZnO, DFT+U, optical band gap, optical properties.

Introduction

The zinc oxide (ZnO) is well known as a wide-band semiconductor with a bandgap = 3.44 eV and exists in the hexagonal wurtzite-type form under normal conditions [1]. The ZnO-based materials have many prospective implementations in various spintronic and optoelectronic devices involving light-emitting diodes, lasers, photodetectors, solar cells, magnetic memory devices, etc. Also, their remarkable structural, electronic, sensor, optical, and electrical properties, together with a large number of different preparation methods appropriate to the production of a high-quality film make them one of the most all-purpose materials in nowadays technology [2]. An efficient method for enhancing the electric and optical characteristics of ZnO is doping them thin film of impurities [3]. Among different kinds of doped ZnO, aluminum-doped ZnO (ZnO: Al) is a cheap, most stable material, has great electric and optical properties, and environmentally friendly, which causes considerable scientific interest. The ZnO: Al has wide possible applications as potential solar cell electrodes [4], transparent conductive oxide, and electrical conductivity [5], optoelectronic and photonic devices [6]. Among numerous techniques of growth of thin films, magnetron sputtering is one of the most favored methods for growing ZnO films because of its simpleness, low operating temperature, and low cost.

In this work, we report experimental and theoretical investigations of the structural and optical properties of Al-doped ZnO thin films. ZnO: Al thin films were synthesized by the magnetron sputtering method. Additionally, we model a 3×3×3 ZnO supercell to perform a theoretical study of Al-doped ZnO using the first-principles method, including examination of electronic structures and optical properties. Using these results, we presented the possibility of using calculated

results to explain experimental data and indicate a definite theoretical direction for the research of ZnO-based doped structures.

I. Experimental details

Al-doped ZnO (ZnO: Al) thin films were deposited on glass substrates with a size of $16\times8\times1.1$ mm^3 by the method of high-frequency (HF) magnetron sputtering (~ 13.6 MHz) using a VUP-5M vacuum station (Selmi, Ukraine) [7, 8]. As a target, the disc from sintered ZnO (purity of 99.99 %) powder with Al2O3 (2.5 wt.%) admixture was used. The target–substrate distance was equal to 60 mm. The start and end of the sputtering process were controlled by means of a movable shutter.

Before the sputtering process, the chamber was pumped out. The gas pressure inside the chamber during the film sputtering was equal to 4×10^{-4} Pa. This pressure is achievable when using a polyphenyl ether (5F4E) as a diffusion fluid in the vapor oil vacuum pump, which possesses a low vapor pressure of 9×10^{-7} Pa.

The power of the HF magnetron was maintained at the level of 30 W and the temperature of the substrate at ~ 373 K. For heating the substrates a high-temperature tungsten heater with a power of 300 W was used. The temperature was controlled using a proportional–integral–derivative (PID) controller for controlling heating and cooling rates, as well as for ensuring the temperature conditions of deposition.

The phase analysis and crystal structure refinement was examined using X-ray diffraction data (XRD) obtained on DRON-2.0M diffractometer at room temperature with the Kα radiation (λ = 1.936087 Å) of Fe.

II. Computational methodology

In this work, the total energies calculations were carried out using the first-principles method within density functional theory (DFT) and implemented in the QUANTUM-ESPRESSO package [9]. Exchange and correlation interactions are described using the generalized gradient approximation (GGA) in combination with ultrasoft pseudopotentials [10]. The considered valence electron are $3d^{10} 4s^2$ for Zn, $2s^2 2p^4$ for O and $3s^2 2p^1$ for Al, respectively. Before property calculations were performed structure optimization of pure and doped ZnO using the Broyden–Fletcher–Goldfarb–Shannon minimizer [11-14]. Well known that GGA suffers from the unavoidable underestimate of bandgap [15], and this difficulty may manipulate the accuracy of the calculated bandgap. To correct the deviation from bandgap many previous works used approximation with Hubbard corrections or the so-called DFT+U [16-18]. When considering calculations for ZnO, GGA underestimates the Zn 3d electrons energy. The top of the valence band forms with the pair Zn d-states and O p-states shifting upwards and essentially narrowing the bandgap [19]. Including the Hubbard U corrections to calculating the insufficient binding of the Zn d electrons lead to adjust the position of the restricted d states and

impacts both the valence band maximum (VBM) and the conduction band minimum (CBM) [16]. In this study were used two Hubbard U corrections: U_d for 3d states of Zn and U_p for 2p states of O. Using two U values which are equal to $U_d = 10$ eV and $U_p = 7$ eV lead to the bandgap of pure ZnO is 3.4 eV which in turn is excellent agreement with experimental data [20]. In this methodology, we were successfully tested on many objects of different dimensions [21-25].

III. Results and discussion

### 3.1. Experimental results

ZnO:Al thin film crystallizes in hexagonal structure (structure type - ZnO, space group $P6_3mc$ (No. 186), with the unit-cell dimensions $a = 3.226(2)$ Å and $c = 5.155(6)$ Å ($V = 46.49(6)$ Å^3). No additional peaks (from X-ray analysis) belonging to other oxides can be detected thereby indicating the formation of pure single ZnO phase, as well as that Al is well incorporated within ZnO lattice.

Then by plotting $(\alpha\cdot h\nu)^2$ versus $h\nu$ (α·is the absorption coefficient and $h\nu$ is the photon energy) one has a possibility to obtain the direct optical band gap E_g from extrapolation of the linear part of the plot to the photon energy axis (see Fig. 1). The estimated optical band gap of the ZnO:Al thin films has been found to be equal to $E_g = 3.26$ eV.

To determine the thickness of the films under investigation, we can use the following equation:

$$d = \frac{M\cdot\lambda_1\cdot\lambda_2}{2\cdot(n(\lambda_1)\cdot\lambda_2 - n(\lambda_2)\cdot\lambda_1)},\qquad(1)$$

where, λ_1 and λ_2 are wavelengths corresponding to neighboring extreme points in the transmission spectrum and $M = 1$ for two neighboring extrema of one type (max–max, min–min) and $M = 0.5$ for two neighboring extrema of opposite types (max-min, min-max). The obtained value of the ZnO: Al thin film thickness is 454.83 nm.
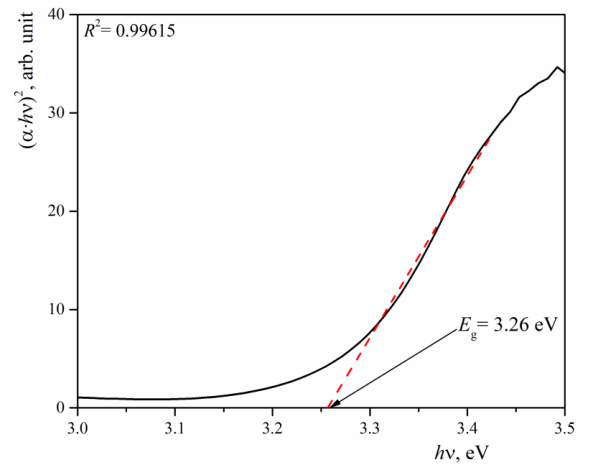
Fig. 1. The spectral dependence of optical absorption for the ZnO:Al thin films.
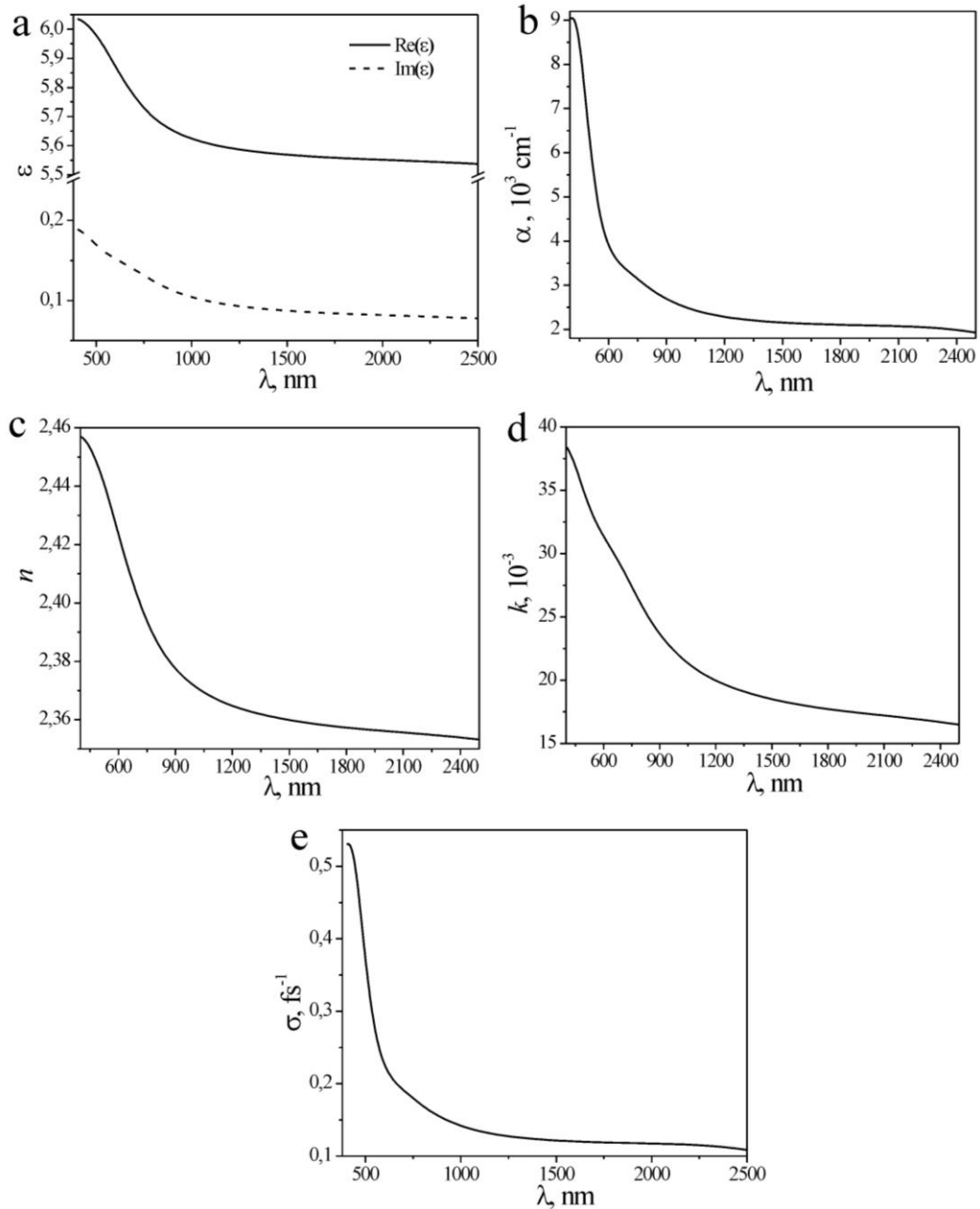
Fig. 2. The dielectric functions (a), absorption coefficient (b), refractive index (c), extinction coefficient (d) and optical conductivity (e) of Al doped ZnO.

The optical properties of a thin film (refractive index $n(\lambda)$, absorption coefficient $\alpha(\lambda)$, extinction coefficient $k(\lambda)$, dielectric functions $\varepsilon(\lambda)$, optical conductivity $\sigma(\lambda)$ and thickness d) can be easily evaluated from a transmission spectrum with interference effects using the envelope method [26-31] (Fig. 2). This method is applicable in the case of a weakly absorbing thin film on an entirely transparent substrate that is much thicker than the thin film. These conditions are met in this work.

3.1. Theoretical results

To analyze the properties of the Al-doped structure was used a 3×3×3 supercell which including 54 Zn atoms and 54 O atoms and present in Fig. 3. In our supercell model, one Zn atom is substituted with one dopant aluminum atom which corresponds to the impurity

concentration close to 1.85 at. %. After structure relaxation the lattice parameters ZnO:Al were $a = b = 3.462$ Å and $c = 5.663$ Å, which are bigger than for pure ZnO ($a = b = 3.251$ Å and $c = 5.213$ [21]). Also, the Zn–O bond lengths for ZnO: Al was 2.08 Å which is longer than those of the pure ZnO (1.98 Å [22]), and the Al–O bond length was 1.86 Å that is shorter than the Zn–O bond lengths. All changes of structure geometry for Al-doped ZnO related to the smaller ionic radius of Al^{3+} (0.54 Å) compared with replaced Zn ion (0.74 Å). The calculated Mulliken population analysis showed that for ZnO:Al the atomic population of Al was 1.60 e and is bigger than of Zn which is 0.94e [22] and indicates that the valence of Al is larger than of Zn. The higher valence of Al also leads to higher values of Al–O bond population (0.47 e) compared with the Zn–O bond

155
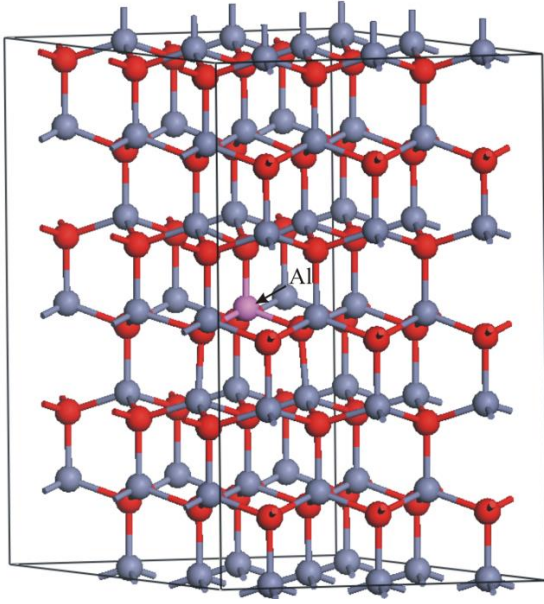
Fig. 3. The supercell model of Al doped-ZnO. Grey, red and pink balls display the zinc, oxygen, and aluminum atoms, respectively.

population of pure ZnO (0.40 *e*).

Next, we investigated the electronic properties of ZnO: Al. The calculated band structure of this model is presented in Fig. 4. The Fermi level is set to 0 eV. The Al-doped ZnO displayed n-type conduction as indicates shifted up into conduction band of the Fermi level, and refers to a well-known effect of the Burstein–Moss [32]. At the bottom of the conduction band, the occupied states can be considered as an additional energy barrier that needed overcome before the electron can be excited from the valence band to the conduction band. This energy barrier is also known as the optical band gap and denotes the energy region from the top of the valence band to the Fermi level. The optical bandgap of the ZnO: Al is 3.43 eV which is bigger than for pure ZnO calculated using the same GGA+U method (3.4 eV [22]). At the same time, it should be noted that the fundamental band gap is 3.3 eV which is smaller compared with undoped ZnO.
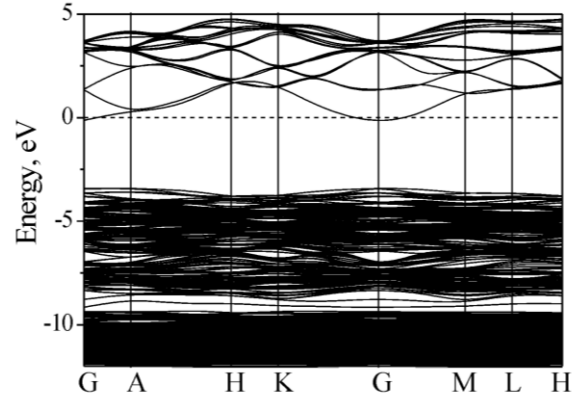

Fig. 4. The band structure of Al doped-ZnO.

Fig. 5a presented the partial density of states (PDOS) of Al-doped ZnO. As can be seen, the calculation results showed the major contribution to the PDOS in the conduction band close by the Fermi level derived from the *s*-orbitals of the Al atom. Moreover, the *s*-contribution in the PDOS at the impurity ion place is considerably larger than that of the Zn atom and leads to an improved electron conductivity of the ZnO: Al (Fig. 5b).

To investigate the optical properties of the ZnO: Al system the dielectric function $\varepsilon(\omega) = \varepsilon_1 + i\varepsilon_2$ was calculated. Ordinarily, the electronic band structure is directly related with $\varepsilon_2(\omega)$ (imaginary part of dielectric function) and it can be calculated by add together all probable occupied states to the unoccupied states of transitions. The $\varepsilon_2(\omega)$ was calculated from the following expression:

$$\varepsilon_2(\omega) = \frac{2e^2\pi}{\Omega\varepsilon_0}\sum_{k,v,c}|\langle\psi_k^c|\hat{u}\times r|\psi_k^v\rangle|\delta(E_k^c - E_k^v - E), \quad (2)$$

where ω is the frequency of light, Ω is the volume of a unit cell, *u* is polarization vector, ψ_k^c and ψ_k^v are the wave functions of valence and conduction bands, respectively. The real part of dielectric function $\varepsilon_1(\omega)$ can be calculated using Kramers-Kronig relation, based on $\varepsilon_2(\omega)$:
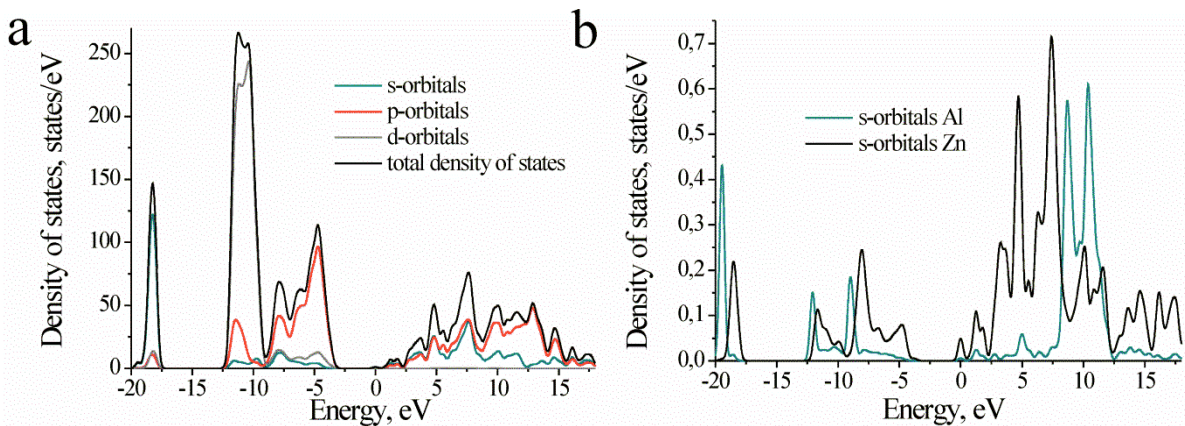
Fig. 5. The partial density of states of Al-doped ZnO (a) and the partial density of s-orbital of Al and Zn (b).

$$\varepsilon_1(\omega) = 1 + \frac{2}{\pi} p \int_0^\infty \frac{\omega' \varepsilon_2(\omega')}{\omega'^2 - \omega^2} d\omega', \quad (3)$$

where p indicates the main value of integral. The other optical functions, e.g. absorption coefficient $\alpha(\omega)$, refractive index $n(\omega)$, extinction coefficient $k(\omega)$ and optical conductivity $\sigma(\omega)$ can be determined by $\varepsilon_1(\omega)$ and $\varepsilon_2(\omega)$ [33].

Fig. 6 displayed the real ε_1 and imaginary part ε_2 of Al-doped ZnO for different polarization vector of light. If compared the theoretical results with the experimental ones presented above (Fig. 2a), we can be seen that the main trend is well consistent with the experimental results. But it is necessary to note the shift of a curve

upwards energy region compared with experimental curves because the difference between experimental and theoretical band gaps received.

The adsorption and conductivity spectrum of Al-doped ZnO is presented in Fig. 7a. As in the case of the dielectric function, the theoretical adsorption spectrum tendency well agrees with the experimental spectrum that is displayed in Fig. 2b. Similar results were obtained in the case of conductivity (Fig. 7b).
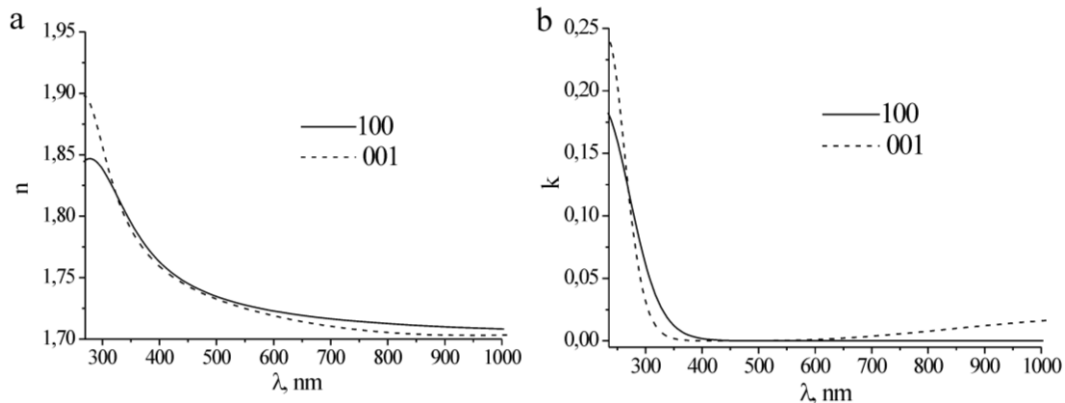
For the full display of experimental results (Fig. 2), we additionally calculated the refractive index and extinction coefficient of Al-doped ZnO that are presented in Fig. 8.
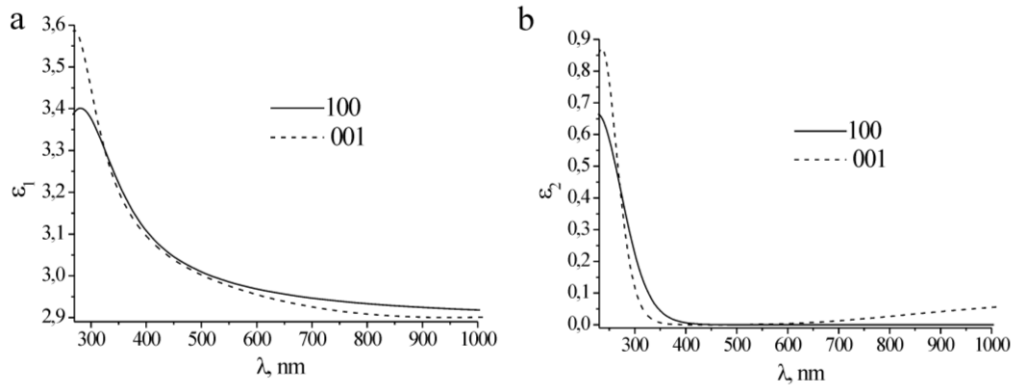
Fig. 6. The real ε_1 (a) and imaginary part ε_2 (b) of Al-doped ZnO.
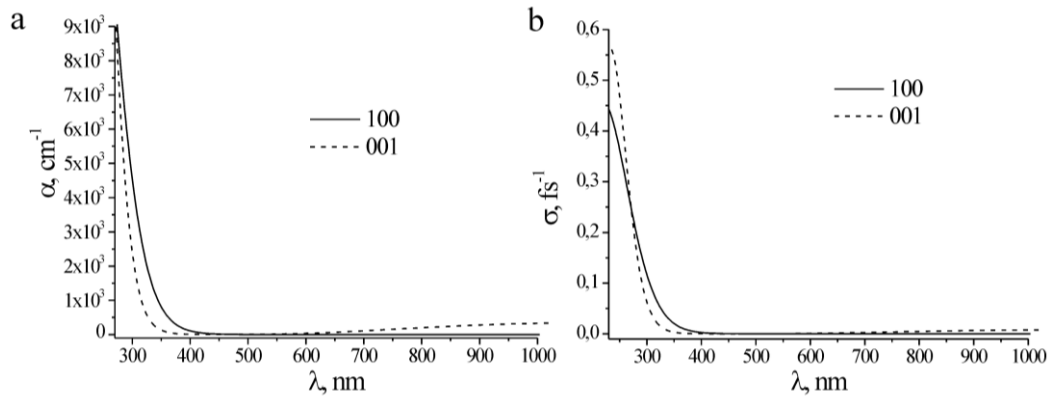
Fig. 7. The adsorption (a) and optical conductivity (b) spectrum of ZnO: Al.

Fig. 8. The refractive index (a) and extinction coefficient (b) of ZnO: Al.

M. Kovalenko, O. Bovgyra, V. Dzikovskyi, A. Kashuba, H. Ilchuk, R. Petrus, I. Semkiv

Conclusions

In this work, the electronic and optical properties of Al-doped ZnO were studied by means of experimental and first-principles calculation approaches. The Al-doped ZnO thin films were grown using the high-frequency magnetron sputtering method. The X-ray analysis approves that the major phase of the prepared samples is the wurtzite structure without secondary phases observed and Al is well incorporated within the ZnO lattice. Additionally, the DFT+U study is used for calculating the band structure of Al-doped ZnO. It was found that adding an Al atom into ZnO enables changes of the ZnO band structure. New states at the top of the valence band, derived from the interaction of valence electrons of Zn, O, and Al atoms. The change of the band structure and PDOS of the ZnO after Al doping means that the doped system may show distinct optical properties. It is important to note that the theoretically obtained results are in good agreement with experimental observations, and the appropriate properties received by calculations for Al-doped ZnO were also established in the actual materials.

Acknowledgements

Kovalenko M. - PhD in Physical and Mathematical Sciences, Associate Professor of Solid-State Physics Department;
Bovgyra O. - PhD in Physical and Mathematical Sciences, Associate Professor of Solid-State Physics Department;
Dzikovskyi V. - PhD student of Solid-State Physics Department;
Kashuba F. - PhD in Physical and Mathematical Sciences, Senior Research Fellow;
Ilchuk H. - Doctor of Physical and Mathematical Sciences, Professor of General Physics Department;
Petrus R. - PhD in Physical and Mathematical Sciences, Associate Professor of General Physics Department;
Semkiv I. - PhD in Physical and Mathematical Sciences, Research Assistant.

[1] C.R.A. Catlow, S.A. French, A.A. Sokol, A.A. Al-Sunadi and S.M. Woodley, J. Comput. Chem. 29, 2234 (2008) (https://doi.org/10.1002/jcc.21051).

[2] Ü. Özgür, Y.I. Alivov, C. Liu, A. Teke, M.A. Reshchikov, S. Do_gan, V. Avrutin, S.-J. Cho, and H. Morkoc, J. Appl. Phys. 98, 041301 (2005) (https://doi.org/10.1063/1.1992666).

[3] Y.S. Lee, Y.C. Peng, J.H. Lu, Y.R. Zhu, H.C. Wu, Thin Solid Films 570, 464 (2014) (https://doi.org/10.1016/j.tsf.2014.04.037).

[4] H. Kumarakuru, D. Cherns and A.M. Collins, Ceramic International 40, 8389 (2014) (https://doi.org/10.1016/j.ceramint.2014.01.045).

[5] V. Devi, M. Kumar and D.K. Shukla, Superlattices and Microstructures 83, 431 (2015) (https://doi.org/10.1016/j.spmi.2015.03.047).

[6] A.A. Al-Ghamdi, O.A. Al-Hartomy and M.El Okr, Spectrochimica Acta Part A: Molecular and Biomolecular Spectroscopy 131, 512 (2014) (https://doi.org/10.1016/j.saa.2014.04.020).

[7] R. Petrus, H. Ilchuk, A. Kashuba, I. Semkiv, E. Zmiiovska, F. Honchar, R. Lys, Journal of Nano- and Electronic Physics 11(3), 03020 (2019). (https://doi.org/10.21272/jnep.11(3).03020).

[8] R.Y. Petrus, H.A. Ilchuk, A.I. Kashuba, I.V. Semkiv, E.O. Zmiiovska, Optics and Spectroscopy 126(3), 220 (2019) (https://doi.org/10.1134/S0030400X19030160).

[9] P. Giannozzi, O. Andreussi, T. Brumme, O. Bunau, M.B. Nardelli, M. Calandra, R. Car, C. Cavazzoni, D. Ceresoli, and M. Cococcioni, J. Phys. Condens. Matter 29, 465901 (2017) (https://doi.org/10.1088/1361-648X/aa8f79).

[10] D. Vanderbilt, Phys. Rev. B 41, 7892 (1990) (https://doi.org/10.1103/PhysRevB.41.7892).

[11] C.G. Broyden, IMA Journal of Applied Mathematics 6(3), 222 (1970) (https://doi.org/10.1093/imamat/6.3.222).

[12] R. Fletcher, The Computer Journal 24(3), 23 (1970) (https://doi.org/10.1093/comjnl/13.3.317).

[13] D. Goldfarb, Mathematics of Computation 24, 23 (1970) (https://doi.org/10.1090/S0025-5718-1970-0258249-6).

[14] D.F. Shanno, Mathematics of Computation 24, 647 (1970) (https://doi.org/10.1090/S0025-5718-1970-0274029-X).

[15] N.N. Lathiotakis, A.N. Andriotis, M. Menon, Phys. Rev. B 78, 193311 (2008) (https://doi.org/10.1103/PhysRevB.78.193311).

[16] R.M. Sheetz, I. Ponomareva E. Richter, A.N. Andriotis, M. Menon, Phys. Rev. B 80, 195314 (2009) (https://doi.org/10.1103/PhysRevB.80.195314).

[17] A. Walsh, J.L.F. Da Silva, S.H. Wei, Phys. Rev. Lett. 100, 256401 (2008) (https://doi.org/10.1103/PhysRevLett.100.256401).

[18] O.V. Bovgyra, M.V. Kovalenko, V.Ye. Dzikovskyi, A.P. Vaskiv, M.Ya. Sheremeta, Journal of Nano- and Electronic Physics 12(5), 05003 (2020) (https://doi.org/10.21272/jnep.12(5).05003).

[19] X. Qu, S. Lü, D. Jia, S. Zhou, Q. Meng, Materials Science in Semiconductor Processing 16(4), 1057 (2013) (https://doi.org/10.1016/j.mssp.2013.04.002).

[20] A. Mang, K. Reimann, St. Rübenacke, Solid State Commun. 94, 251 (1995). (https://doi.org/10.1016/0038-1098(95)00054-2).

[21] O. Bovgyra, M. Kovalenko, R. Bovhyra, V. Dzikovskyi, Journal of Physical Studies 23(4), 4301 (2019) (https://doi.org/10.30970/jps.23.4301).

[22] M. Kovalenko, O. Bovgyra, A. Franiv, V. Dzikovskyi, Materials Today: Proceeding (2019) (https://doi.org/10.1016/j.matpr.2019.11.274).

[23] O. Bovgyra, M. Kovalenko, V. Dzikovskyi, and M. Moroz, IEEE 2nd Ukraine Conference on Electrical and Computer Engineering (UKRCON), (Lviv, Ukraine, 2019), p. 726 (https://doi.org/10.1109/UKRCON.2019.8879928).

[24] O.V. Bovgyra and M.V. Kovalenko, Journal of Nano- and Electronic Physics 8(2), 2031 (2016) (https://doi.org/10.21272/jnep.8(2).02031).

[25] M.V. Kovalenko, O.V. Bovgyra, V.Ye. Dzikovskyi, R.V. Bovhyra, Nanosistemi, Nanomateriali, Nanotehnologii 18(3), 727 (2020).

[26] L.I. Nykyruy, R.S. Yavorskyi, Z.R. Zapukhlyak, G. Wisz, P. Potera, Optical Materials 92, 319 (2019) (https://doi.org/10.1016/j.optmat.2019.04.029).

[27] R.Yu. Petrus, H.A. Ilchuk, A.I. Kashuba, I.V. Semkiv, E.O. Zmiiovska, F.M. Honchar, Journal of Applied Spectroscopy 87(1), 35 (2020) (https://doi.org/10.1007/s10812-020-00959-7).

[28] R. Petrus, H. Ilchuk, A. Kashuba, I. Semkiv, E. Zmiiovska, Funct. Mater. 27(2), 342 (2020) (https://doi.org/10.15407/fm27.02.342).

[29] R. Yavorskyi, L. Nykyruy, G. Wisz, P. Potera, S. Adamiak and Sz.Górny, Applied Nanoscience (Switzerland) 9, 715 (2018) (https://doi.org/10.1007/s13204-018-0872-z).

[30] H. Ilchuk, R. Petrus, A. Kashuba, I. Semkiv and E. Zmiiovska, Molecular Crystals and Liquid Crystals 699(1), 1 (2020) (https://doi.org/10.1080/15421406.2020.1732532).

[31] A. Kashuba, H. Ilchuk, R. Petrus, I. Semkiv, O. Bovgyra, M. Kovalenko and V. Dzikovskyi, Modern Physics Letters B 33, 2150189 (2021) (https://doi.org/10.1142/S021798492150189X).

[32] R. Ebrahimifard, M.R. Golobostanfard, H. Abdizadeh, Applied Surface Science 290, 252 (2014) (https://doi.org/10.1016/j.apsusc.2013.11.062).

[33] S. Saha, T.P. Sinha, A. Mookerjee, Physical Review B: Condensed Matter 62, 8828 (2000) (https://doi.org/10.1103/PhysRevB.62.8828).

М. Коваленко[1, 2], А. Кашуба[2], О. Бовгира[1], В. Дзіковський[1, 2], Г. Ільчук[2], Р. Петрусь[2], І. Семків[2]

Вплив легування атомів Al на оптичні властивості тонких плівок ZnO: теорія та експеримент

[1]Львівський національний університет імені Івана Франка, Львів, Україна, mariya.kovalenko@lnu.edu.ua
[2]Національний університет «Львівська Політехніка», Львів, Україна, andriykashuba07@gmail.com

Проведено дослідження впливу легування атомами алюмінію на структурні, електронні і оптичні властивості тонких плівок оксиду цинку, використовуючи експериментальні методи та розрахунки в межах теорії функціонала густини. Зміни властивостей легованих тонких плівок, які були нанесенні на скляну підкладку методом високочастотного магнетронного розпилення, контролювалися за допомогою даних Х-променевої дифракції та спектрів пропускання. Результати теоретичних розрахунків показують, що електронна структура ZnO:Al добре узгоджується з експериментальними даними при використанні методу DFT + U. На основі спектрів пропускання визначено оптичні константи для легованих плівок, такі як діелектрична проникність, показник заломлення, ширина оптичної забороненої зони, коефіцієнт екстинкції та оптична провідність. Результати розрахунків показали, що при внесенні домішкового атома Al в суперкомірку ZnO, спостерігається зміна параметрів цієї гратки. Ширина оптичної забороненої зони ZnO:Al зростає порівняно з нелегованим ZnO. Крім того, навколо рівня Фермі, в ZnO:Al, виникають неглибокі донорні рівні, які переважно походять від 3s-орбіталей Al. Результати наших розрахунків оптичних властивостей ZnO, легованого Al, в межах DFT, задовільно узгоджуються з експериментально виміряними значеннями коефіцієнта пропускання.

Keywords: легований ZnO, DFT+U, ширина оптичної забороненої зони, зонно-енергетична структура, оптичні властивості.